3. SUPERNOVAE

https://doi.org/10.1017/S0252921100086048 Published online by Cambridge University Press

The Physics of Supernovae

S. E. Woosley
Board of Studies in Astronomy and Astrophysics
Lick Observatory, University of California at Santa Cruz
Santa Cruz CA 95064
and
Special Studies Group, Lawrence Livermore National Laboratory
Livermore CA 94550
and
Thomas A. Weaver
Special Studies Group, Lawrence Livermore National Laboratory
University of California, Livermore CA 94550

Abstract

Presupernova models of massive stars are presented and their explosion by "delayed neutrino transport" examined. A new form of long duration Type II supernova model is also explored based upon repeated encounter with the electron-positron pair instability in stars heavier than about 60 $M_\odot$. Carbon deflagration in white dwarfs is discussed as the probable explanation of Type I supernovae and special attention is paid to the physical processes whereby a nuclear flame propagates through degenerate carbon.

1. INTRODUCTION

Few phenomena in nature are so direct and spectacular a consequence of hydrodynamics and radiation transport as the explosion of a supernovae. Type II supernovae, now recognized as the endpoints of stars of some 9 $M_\odot$ or more, occur when the inert iron core collapses to nuclear density, bounces like a rubber ball, and generates an outgoing shock wave that either leads directly to the explosion or gives rise to a situation in which energy transport by neutrinos can unbind the region external to the core. Type I supernovae on the other hand, entirely a separate and distinct occurrence so far as the theoretician is concerned, are enormous thermonuclear explosions of degenerate white dwarf stars that have accreted a critical mass, explosions that, were it not for the energy stored in the form of slowly decaying radioactive isotopes, would be almost totally invisible optically. Somewhat surprisingly, the total energy release in both varieties of supernova, $\sim 10^{51}$ erg, is comparable. This is because of the relative inefficiency of coupling the large energy ($\sim 10^{53}$ erg) released in the gravitational collapse of a stellar core to a neutron star to its more loosely bound extremities (the rest escapes as neutrinos) compared to the almost completely efficient coupling of a less energetic power source, nuclear reactions in an exploding white dwarf.

Observations agree with the general properties expected of these models. Type II's, since they are associated with massive young stars, are not seen in elliptical galaxies (Tammann 1974) but are found, although not uniquely, in the spiral arms of spiral galaxies (Maza and van den Bergh 1976). Type I supernovae, on the other hand, are characterized, as an exploding white dwarf should be, by a lack of hydrogen lines in their spectra. Furthermore they occur in all varieties of galaxies since it may take a Hubble time to accrete the critical mass. Presently, in our Galaxy, Type II supernovae are estimated to occur every 44 years and Type I's every

https://doi.org/10.1017/S0252921100086048 Published online by Cambridge University Press

36 years (Tammann 1982) though the optical emissions of most are heavily obscured by dust.

The basic physics involved in both types of supernovae has been recognized for at least 10 years, but a definitive solution, acceptable to the majority of those working in the field, has been long in coming. Distinct difficulties beset models for each type. In the case of a massive star whose iron core collapses to nuclear density and bounces, the complex coupling of neutrino energy transport, nuclear physics, and hydrodynamics in a situation where marginal changes in the physical parameters cause large variation in the outcome poses difficult computational problems as well as taxes the accuracy with which key quantities, *e.g.* the pressure and energy of matter at nuclear density, the exact presupernova stellar configuration, and the magnitude of rotation and magnetic fields, are known. For a Type I supernova, the specific evolutionary scheme that results in a white dwarf approaching the Chandrasekhar mass in a binary system is still debatable (Iben and Tutukov 1984, 1985; Webbink 1984), especially given the additional complexity introduced by the nova instability.

Challenging and controversial too is the nature of the nuclear flame that propagates through the dwarf and energizes the explosion. In various white dwarfs and, perhaps even at various stages in the same star this front may move by conduction, detonation, or, most importantly, turbulence. The flame leaves behind as its major ash the radioactive isotope ^{56}Ni. Energy released at late times by the decay of this ^{56}Ni and its daughter ^{56}Co is initially in the form of γ-rays and relativistic positrons but is rapidly degraded into emission, chiefly in the optical, by atomic processes of which we have only recently become cognizant (Meyerott 1980; Axelrod 1980ab). The transport of this radiation in a differentially expanding atmosphere in which a forest of iron and cobalt lines spread out by Doppler broadening so as to mimic a continuum is a frontier problem in numerical astrophysics, currently taxing the largest computers and most intricate codes available (Harkness, this volume; Pinto and Axelrod 1986).

In this paper we briefly review some of the current attempts to model Type I and II supernova explosions and discuss several perplexing problems facing the theoretician. Some of the material presented here has also been treated in other recent reviews (Wilson *et al* 1985; Woosley and Weaver 1985, 1986a) and receives only cursory attention. However, three important new results are presented for the first time: 1) the pulsational pair instability for repetitive, *enduring* supernova outbursts (§2.5), 2) a summary of the elemental nucleosynthesis of intermediate mass elements over the entire stellar mass range studied ($12 \lesssim M/M_{\odot} \lesssim 100$) in the presupernova star (§2.2), and 3) new insights into the nature of the nuclear flame and its propagation in a Type I supernova (§3.2, 3.3, and 3.4). The *aficianado* already familiar with our other recent work may wish to proceed directly to those sections.

2. TYPE II SUPERNOVAE

2.1 Presupernova Evolution of Massive Stars

The mass range for supernovae fitting our generic description of Type II is bounded on the lower end by the heaviest stars that can become white dwarfs and on the upper end by the most massive star that retains its hydrogen envelope at the time its core explodes. Stars having still greater mass exist (Humphreys 1984; Massey 1981) and may explode but, lacking a hydrogen envelope, both their light curves and spectra would disqualify them for the label "Type II" (Chevalier 1976; Woosley and Weaver 1982a; Fillipenko and Sargent 1985). For single stars, the progenitor of the heaviest white dwarf has a mass on the main sequence that,

https://doi.org/10.1017/S0252921100086048 Published online by Cambridge University Press

depending on helium abundance, metallicity, and convection model is near 8 or 9 $M_\odot$, (Iben and Renzini 1983, although see Berteli, Bressan, and Chiosi 1985). This value is consistent with statistical arguments on the occurrence of supernovae (Tammann 1982), the preferential location of Type II's in spiral arms (Maza and Van den Bergh 1976), observations of white dwarfs (Romanishin and Angel 1980; Weidemann and Koester 1983), and theoretical models for white dwarf formation (Iben 1985). Above 9 $M_\odot$, the star will ignite carbon burning non-degenerately and avoid the development of a thin helium burning shell which may be instrumental in envelope ejection (Tuchmann, Sack, and Barkat 1979).

The most massive star that dies while still in possession of its hydrogen envelope is uncertain and probably depends upon metallicity. Estimates range from about 20 $M_\odot$ (Chiosi 1981; Firmani 1982; Berteli, Bressan, and Chiosi 1984) to more than 40 $M_\odot$ (Conti, Leep, and Perry 1983, although see Utrobin 1984 for a special exception) with a favored value around 40 $M_\odot$ (Schild and Maeder 1983; Maeder 1984). Such stars as η-Car, S-Dor, P-Cygni, and the Hubble-Sandage variables may exemplify the transition to the Wolf-Rayet stage (Humphreys 1984; Lamers, DeGroot and Cassatella 1983). Though of interest for their nucleosynthesis, for the properties of their collapsed remnants, and for the special optical (or *UV*?) properties their explosions may exhibit, such stars are relatively rare and would not contribute appreciably ($\lesssim$10%) to the present Type II supernova sample.

It is useful to segregate the remaining progenitors into two subclasses, 9 to 12 $M_\odot$ and everything else (Barkat, Reiss, and Rakavy 1974). The former is a transitional region bounded on the lower end by stars that ignite carbon degenerately and on the upper end by those that ignite all six nuclear burning stages: hydrogen, helium, carbon, neon, oxygen, and silicon burning, non-degenerately in their center. In this intermediate mass region the late stages of stellar evolution can be quite complicated because the high density and near degeneracy of the gas lead to off-center burning and because electron capture is important to the structure of the star.

Stars in the 9 to 12 $M_\odot$ range have been recently examined by Nomoto (1984ab, 1985), Hillebrandt, Nomoto and Wolff (1984), Woosley, Weaver, and Taam (1980), and Wilson *et al* (1985) and several aspects of the presupernova star warrant special mention. First, because low mass stars are more common than heavier ones, even this narrow range, which may be 8 (or even less; Berteli, Bressan, and Chiosi 1985) to 12 $M_\odot$ or 9 to 11 $M_\odot$ depending on uncertain parameters, may provide a large fraction of the observed Type II supernovae. Second, because of their near degeneracy, or alternatively their small central entropies, the presupernova stars have, at the time of core collapse, thin shells of heavy elements surrounding a core of nearly the Chandrasekhar mass (as modified by electron capture). Thus, even though they may be common, they create little in the way of heavy element nucleosynthesis. The Crab Nebula may be an example of such an explosion. Finally, for the same reason, the iron core that collapses in a star in this mass range is as small as one can hope to get. Larger stars that are less degenerate, that have higher central entropies, will not converge on a core mass so close to the Chandrasekhar value. Since it is very difficult to make a large iron core explode promptly by the shock wave from its bounce at nuclear density, it is only stars in or near the 8 to 12 (or maybe 15) $M_\odot$ range that presently appear promising candidates for explosion by the core bounce mechanism (Baron, Cooperstein, and Kahana 1985ab).

2.2 Presupernova Models in the 12 to 50 $M_\odot$ Range

We have recently computed a number of presupernova models in the 12 to 50 $M_\odot$ mass range,

https://doi.org/10.1017/S0252921100086048 Published online by Cambridge University Press

several of which have been previously discussed by Woosley and Weaver (1985) and Wilson *et al* (1985). The results are summarized in Figures 1 and 2 and Tables 1 and 2. Table 1 gives, for each main sequence mass, the size of the helium core at the time the iron core collapses. This mass is sensitive, among other things, to the initial helium abundance assumed. The present study adopted 0.21 (Cameron 1982), a value that, in retrospect, is too small. For a more reasonable helium abundance, $Y = 0.28$, the various helium core masses should be multiplied by ~1.1. Thus the 25 $M_\odot$ model would have a helium core of 9.4 $M_\odot$, closer to the value obtained by Weaver, Zimmerman, and Woosley (1978), and so on. The iron core mass is that region composed of iron group isotopes at the time the collapse velocity reaches 1000 km s^{-1} at any point. Other definitions of "core mass," *e.g.* the point where the density suddenly declines (Figure 1) or the point where the total entropy increases suddenly by a large factor, would give slightly different and generally larger values. The 75 and 100 $M_\odot$ models become unstable at oxygen ignition and are discussed separately in §2.5. The column labeled "Heavies Ejected" refers to that region interior to the helium burning shell but exterior to the iron core. The other three entries are properties of "delayed explosions" (§2.3) calculated by Wilson *et al* (1985). Note that the gravitational mass of the neutron star differs from the residual mass immediately following explosion because of the 10 to 25% of the mass energy ultimately lost to neutrino emission, *i.e.*, the gravitational binding energy of the cold neutron star.

TABLE 1

PRESUPERNOVA MODELS AND EXPLOSIONS

Main Seq. Mass	Helium Core Mass	Iron Core Mass	Expl. Energy[a] (10^{50}erg)	Residual Baryon Mass[a]	Neutron Star Mass[a]	Heavies Ejected ($Z \geq 6$)
11	2.4	—[b]	3.0	1.42	1.31	~0
12	3.1	1.31	3.8	1.35	1.26	0.96
15	4.2	1.33	2.0	1.42	1.31	1.24
20	6.2	1.70	—	—	—	2.53
25	8.5	2.05	4.0	2.44	1.96	4.31
35	14	1.80	—	—	—	9.88
50	23	2.45	—	—	—	17.7
75	36	—[c]	—	—	BH?	30?
100	45	~2.3[c]	≳4	—	BH?	39?

[a] All except for 100 $M_\odot$ determined by Wilson *et al* (1985).

[b] Never developed iron core in hydrostatic equilibrium.

[c] Pulsational pair instability at oxygen ignition.

All these models were computed using the current, though still controversial, rate for the reaction $^{12}C(\alpha,\gamma)^{16}O$ (Langanke and Koonin 1983, 1985), a parameter to which the iron core masses as well as nucleosynthesis are very sensitive. Note also a non-monotonic behavior in the iron core mass between 25 and 50 $M_\odot$ owing to variations in the number of shell oxygen burning episodes experienced by the star before its core collapses.

Table 2 gives the presupernova nucleosynthesis, in solar masses, of the elements heavier than carbon. The second row in each case normalizes the production to solar values relative

https://doi.org/10.1017/S0252921100086048 Published online by Cambridge University Press

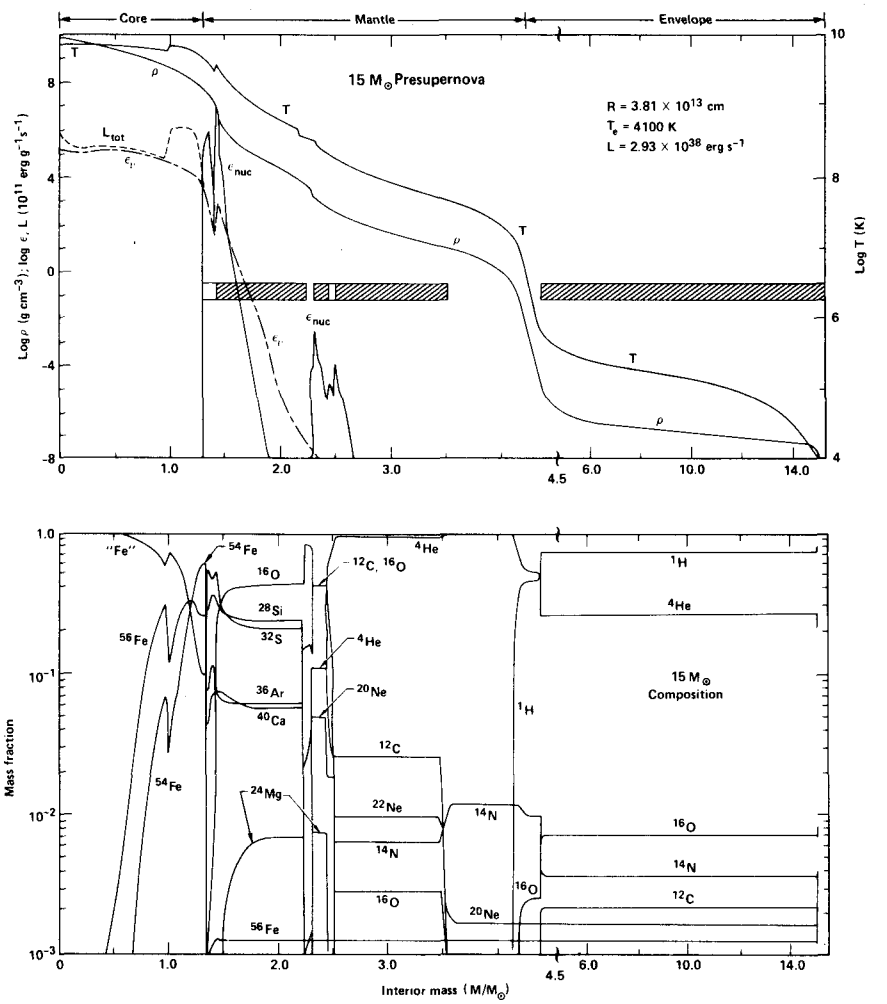

Figure 1. Structure and composition of a 15 $M_\odot$ presupernova star at a time when the edge of its iron core begins collapsing at 1000 km s^{-1}. Neutrino emission from electron capture (ϵ_ν) dominates photodisintegration in the total energy losses (L_{tot}) throughout most of the iron core. Central temperature here is 7.62×10^9K and density, 9.95×10^9 g cm^{-3}. Spikes in the nuclear energy generation rate (ϵ_{nuc}) show the location of active burning shells while cross-hatched, blank, and open bars indicate regions that are convective, semi-convective, and radiative respectively. The species "Fe" includes all isotopes from $48 \lesssim A \lesssim 65$ having a neutron excess greater than ^{56}Fe. Note a scale break at 4.5 $M_\odot$. Figure adapted from Woosley and Weaver (1985).

https://doi.org/10.1017/S0252921100086048 Published online by Cambridge University Press

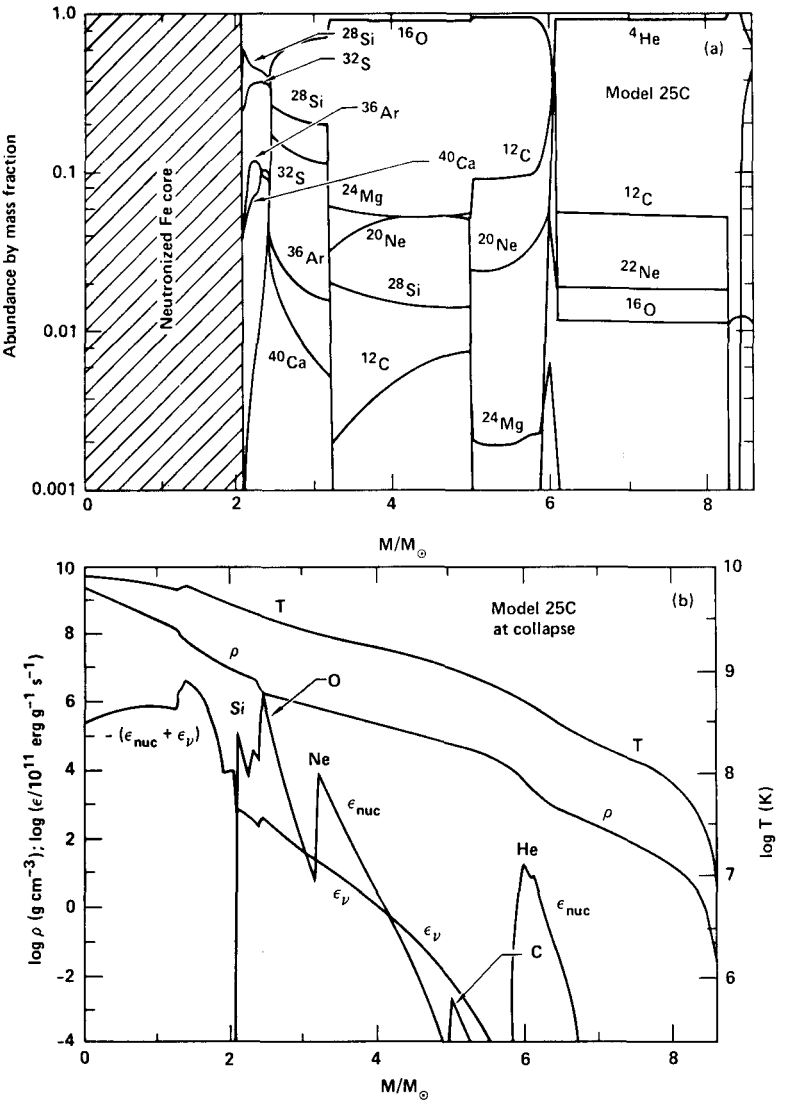

Figure 2. Composition of the inner regions of a 25 $M_\odot$ star at the onset of core collapse (as defined in Fig. 1). Interior to the iron core (2.05 $M_\odot$) energy is being lost due to a combination of neutrino emission from electron capture and photodisintegration. The density falls off rapidly just outside the iron core. Note the larger iron core than in the 15 $M_\odot$ model and the less steep decline of density outside the core. A substantial fraction of the silicon shell shown here will accrete onto the neutron star before an explosion finally occurs. Figure taken from Wilson *et al* (1985).

https://doi.org/10.1017/S0252921100086048 Published online by Cambridge University Press

to oxygen. Some of these abundances will experience considerable modification in the ejection process (§2.4). Elements from carbon through aluminum, being located fairly far out in the star (Figs. 1 and 2) are not particularly sensitive to the mechanism of the explosion, so long as one occurs. Elements heavier than silicon on the other hand may experience substantial alteration, in part owing to explosive processing as the shock wave moves through, but also by accreting onto the incipient neutron star. This latter effect is especially important in the delayed explosions of the more massive stars, which are, of course, the major contributors to galactic nucleosynthesis. Note, for example, the difference between "Iron Core Mass" and "Residual Baryon Mass" (Table 1) in the 25 $M_\odot$ model. This is chiefly silicon shell material that accretes before the explosion gets going. The loss aids in reducing the large overproductions of the intermediate mass elements now characterizing the presupernova models.

TABLE 2
PRESUPERNOVA NUCLEOSYNTHESIS

Mass ($M_\odot$)	^{12}C	^{16}O	^{20}Ne	^{24}Mg	^{28}Si	^{32}S	^{36}Ar	^{40}Ca
12[a]	0.070	0.46	0.040	0.039	0.22	0.088	0.016	0.026
[b]	0.34	1	0.56	1.3	5.5	3.7	3.2	6.9
15	0.13	0.50	0.034	0.012	0.22	0.23	0.059	0.054
	0.57	1	0.43	0.35	5.1	8.7	11	13
20	0.21	1.6	0.058	0.023	0.34	0.22	0.043	0.022
	0.29	1	0.23	0.21	2.4	2.6	2.4	1.6
25	0.26	3.1	0.18	0.11	0.37	0.23	0.054	0.037
	0.19	1	0.38	0.52	1.4	1.5	1.6	1.5
35	0.30	6.4	0.90	0.16	1.1	0.84	0.18	0.20
	0.10	1	0.89	0.37	1.9	2.5	2.2	3.7
50	0.31	12	0.78	0.66	2.1	1.5	0.45	0.23
	0.058	1	0.43	0.84	2.1	2.5	3.5	2.4
100	0.78	30	1.5	1.2	3.3	1.8	0.31	0.27
	0.057	1	0.32	0.59	1.3	1.1	0.9	1.1

[a] Mass in solar masses at time of core collapse

[b] Production normalized to oxygen in the sun.

The *aficionado* will note that these large productions of intermediate mass elements did not exist in our earlier presupernova models (Weaver, Zimmerman, and Woosley 1978; Weaver, Woosley, and Fuller 1984). They are entirely a consequence of recent experimental inflation of the reaction rate for $^{12}C(\alpha,\gamma)^{16}O$ and its effect on the presupernova convective shell structure (Woosley and Weaver 1985; 1986a). The same is also true of the diminished neon and magnesium abundances. Both are products of carbon burning.

2.3 Core Collapse and Explosion in $M \lesssim 50\ M_\odot$

For many years the outward propagation of the shock wave produced by the bounce of these iron cores has been studied as a possible mechanism for the explosion (*cf.* Bowers and Wilson 1982; Arnett 1983; Brown, Bethe, and Baym 1982; Hillebrandt 1984; Bruenn 1985; Baron,

https://doi.org/10.1017/S0252921100086048 Published online by Cambridge University Press

Cooperstein, and Kahana 1985ab). For the most part, the results of these studies have not been particularly encouraging, except, perhaps, in the case of the low mass iron cores characterizing the 9 to 15 $M_\odot$ stars (Table 2; Hillebrandt, Nomoto, and Wolff 1984; Baron, Cooperstein, and Kahana 1985ab). Currently it is controversial whether a prompt ($\lesssim$20 ms), hydrodynamical explosion will give a supernova explosion even in this restricted mass range. The outcome is sensitive to uncertain details of the nuclear equation of state, a "softer" EOS (Baron *et al* 1985) favoring explosion.

In many calculations (Bowers and Wilson 1982; Wilson *et al* 1985; Bruenn 1985; Burrows and Lattimer 1985) prompt hydrodynamical explosions do not occur, even for the lower mass stars/cores, and certainly not for the large cores characterizing stars of $M \gtrsim 20$ $M_\odot$. The shock stalls, overwhelmed by photodisintegration and neutrino losses, and becomes a nearly stationary accretion shock. This may not be the end of the story however. More recently, slow late time heating of the envelope of the incipient neutron star has been found to be capable of rejuvenating the stalled shock. The slow accumulation of energy behind the accretion shock, absorbed in a region optically thin to neutrinos, leads to gradual heating and expansion, ultimately producing an explosion (Wilson 1985a; Bethe and Wilson 1985; Wilson *et al* 1985; Mayle 1985). The following explanation of this behavior, first observed in numerical calculations by Wilson (1985a), has been given by Bethe and Wilson (1985).

A few hundredths of a second following bounce, matter from the outer parts of the core and the surrounding stellar mantle is falling nearly freely onto an almost stationary accretion shock. Below the shock matter settles inward relatively slowly and accumulates on the dense core (Fig. 3). The heating rate of the slowly settling, optically thin (to neutrinos) matter at a radius $r \sim 10^7$ cm is given approximately by

$$\begin{aligned} \dot{E}_+ &= \kappa_a(T_p)\ (L_\nu Y_n\ + L_{\bar{\nu}} Y_p)/4\pi r^2 \\ &\approx \kappa_a(T_p)\ L_\nu/4\pi r^2 \end{aligned} \tag{1}$$

where $L_\nu \approx L_{\bar{\nu}}$ at late times and matter is presumed to be dissociated into free nucleons in the region of interest. Here κ_a is the absorption opacity, given chiefly by neutrino capture on nucleons, T_p, the neutrinosphere temperature, L_ν, the electron neutrino luminosity, and r, the radius. Heating due to electron scattering is initially small and is ignored here. The cooling rate of the matter on the other hand is

$$\dot{E}_- = \kappa_e(T_m) a' c T_m^4 \tag{2}$$

where κ_e is the emission opacity due to interactions that are the inverse of those giving κ_a, *i.e.*, electron and positron capture on nucleons, T_m is the local matter temperature, and a' is the radiation constant for neutrinos ($\frac{7}{16}$ of the photon radiation constant).

The matter in the region of interest is only moderately degenerate, thus

$$\begin{aligned} \kappa_a &= 1.33\ \sigma_0 (\frac{\epsilon_\nu}{m_e c^2})^2 / m_H \\ &\approx 11.0 \times 10^{-19} T_p^2\ \mathrm{cm}^2\ \mathrm{g}^{-1}. \end{aligned} \tag{3}$$

Similarly $\kappa_e = 11.0 \times 10^{-19}\ T_m^2$ with both temperatures measured in MeV. One can also approximate the luminosity of the neutrinosphere as that of a modified blackbody

$$\begin{aligned} L_\nu &\approx 4\pi r_p^2 a' c T_p^4/4, \\ \dot{E}_{net} &\approx 2.0 \times 10^{18}\ T_p^6 \left[(\frac{r_p}{2r_m})^2 - (\frac{T_m}{T_p})^6 \right]\ \mathrm{erg\ g^{-1} s^{-1}}. \end{aligned} \tag{4}$$

https://doi.org/10.1017/S0252921100086048 Published online by Cambridge University Press

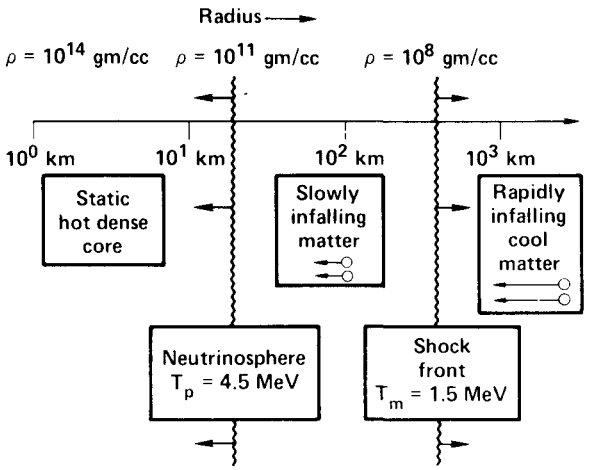

Figure 3. Schematic representation of the conditions that exist near the collapsed core of a massive star a few tenths of a second following the collapse. The neutrinosphere is slowly shrinking in radius as the material beneath it cools. The accretion shock is moving outwards owing to the deposition of neutrino energy in the material just beneath. Figure taken from Wilson *et al* (1985).

Thus once the temperature of matter behind the accretion shock has declined to $T_m < T_p$ $(r_p/2r_m)^{1/3}$ net heating will dominate. For a core mass of 1.5 $M_\odot$, the gravitational energy is $2 \times 10^{19}/r_7$ ergs g^{-1}, with r_7 the radius in units of 10^7 cm, which is also approximately the internal energy of the material in the region of interest. The low density of matter there implies that the nuclei will disintegrate even at temperatures so low as 1 to 2 MeV. This requires an energy of about 8×10^{18} ergs g^{-1}. If the entropy in this region is low, less than $10k$, the degeneracy of the electrons may be an important sink of energy, and if the entropy is high, pairs and radiation are big sinks of energy. Thus, the heat capacity of matter in this region is large and the temperatures stay moderately low. Furthermore the heating, which absorbs typically $\lesssim$1% of the neutrino flux flowing through the matter, does not decrease significantly (eq. 4) as the matter expands until a large fractional change in r_p has occurred. Thus moderate expansion does not quench the instability and an explosion can occur. Important too in this regard is a fall off in the ram pressure, ρv^2, of the infalling material as the silicon shell is accreted and one arrives at what was the base of the oxygen burning shell in the presupernova star (Figs. 1 and 2). This also reduces the photodisintegration losses that must be provided by the shock. Generally the explosion of the more massive stars occurs at this time. Typically $T_p \sim 4.5$ MeV, $r_p \sim 30$ km, and $\dot{E}_{net} \sim 5 \times 10^{20}/r_7^2$ erg g^{-1} s^{-1}. The local gravitational binding energy is of order 2×10^{19} erg g^{-1} implying an explosion time scale of a few hundredths of a second. In practice the accreting material plays an important role and the explosion time scale is longer, a few tenths of a second. For a more detailed discussion of the heating process see Bethe and Wilson (1985), Wilson *et al* (1985), and Mayle (1985). Figure 4 shows the delayed explosion of the 25 $M_\odot$ model given in Figure 2 and Table 1.

https://doi.org/10.1017/S0252921100086048 Published online by Cambridge University Press

Since the supernova is energized, in this scenario, by the absorption of a small fraction of the neutrino flux streaming from the core, it is clear that an increase in this flux would favor a more energetic and robust explosion. Recently it has been realized that *convection* at late times may be instrumental in boosting the flux. That portion of the core just beneath the neutrinosphere may be convectively unstable for a variety of reasons: "salt-finger" instability owing to a gradient in lepton number; entropy gradient due to a weakening of the shock as it propagated through the core; and neutrino losses from the surface of the core leading to a positive entropy gradient. All are currently under investigation (Arnett 1985; Bowers 1985; Bethe 1985; Mayle 1985). Since the energy of the explosions obtained thus far by the "delayed mechanism" have been less energetic than one would like (Table 1) and since not all model builders even agree that the mechanism works at all (Hillebrandt 1985; Arnett 1985), these studies will be very important in determining whether the elusive solution to the Type II supernova problem has finally been found.

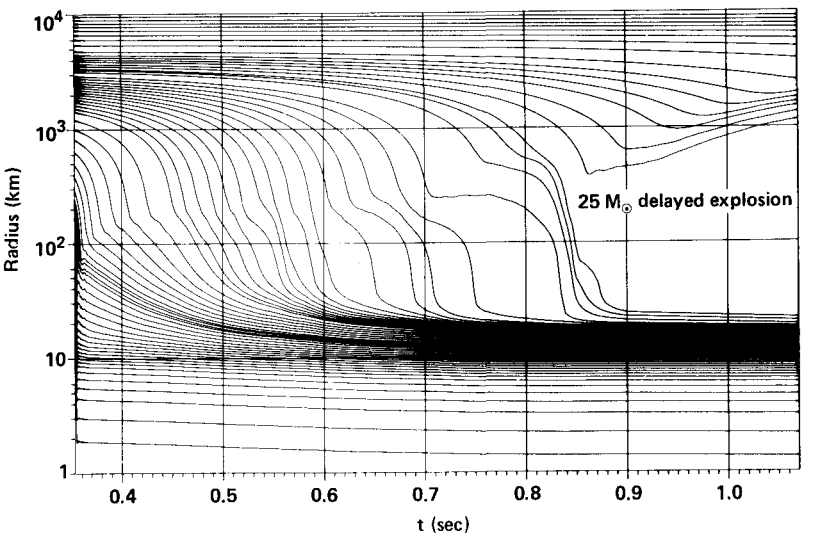

Figure 4. Radius as a function of time for the 25 $M_\odot$ delayed explosion calculated by Wilson *et al* (1985). Time is measured from the onset of core collapse, bounce occurring here at 0.35 s. Note one or more episodes (*e.g.* $\sim$ 0.75 s) when an explosion almost occurs but is overwhelmed by infalling matter. Explosion finally does occur when the density of the accreting matter sharply declines (Fig. 2).

2.4 Explosive Nucleosynthesis in Type II Supernovae

The passage of the shock wave through the overlying mantle of the star, in addition to providing the impulse for its ejection, leads to high temperatures and nuclear reactions that were followed in detail for the 25 $M_\odot$ model (Wilson *et al* 1985, Model 25C). Figure 5 shows the resultant isotopic nucleosynthesis. The comparison with solar abundances is very good, much better, for example, we published for a previous 25 $M_\odot$ model (Woosley and Weaver 1982b).

https://doi.org/10.1017/S0252921100086048 Published online by Cambridge University Press

The changes reflect principally the altered structure of the presupernova mantle and core brought about by revisions in weak interaction rates (Weaver, Woosley, and Fuller 1985) and in the reaction rate for $^{12}C(\alpha,\gamma)^{16}O$. It is worth noting that 34 species out of a total of 61 in this mass range are produced within a factor of two of their relative solar abundances and 52 are produced within a factor of 4. In the sun these abundances span a range in mass fraction of 7 orders of magnitude. Of the remaining 9, ^{13}C and ^{15}N are probably the products of hydrogen burning in lower mass red giant stars and novae respectively; the origin of fluorine is unknown; ^{18}O is produced in a 15 $M_\odot$ star to be reported elsewhere; ^{46}Ca and ^{47}Ti are very rare species whose production might be quite sensitive to poorly determined nuclear reaction rates (or a change in stellar mass); ^{48}Ca and ^{54}Cr can be made in a neutron-rich nuclear statistical equilibrium (Hartmann, Woosley, and El Eid 1985); and ^{63}Ni was near the end of our nuclear reaction network and may not have been tracked accurately.

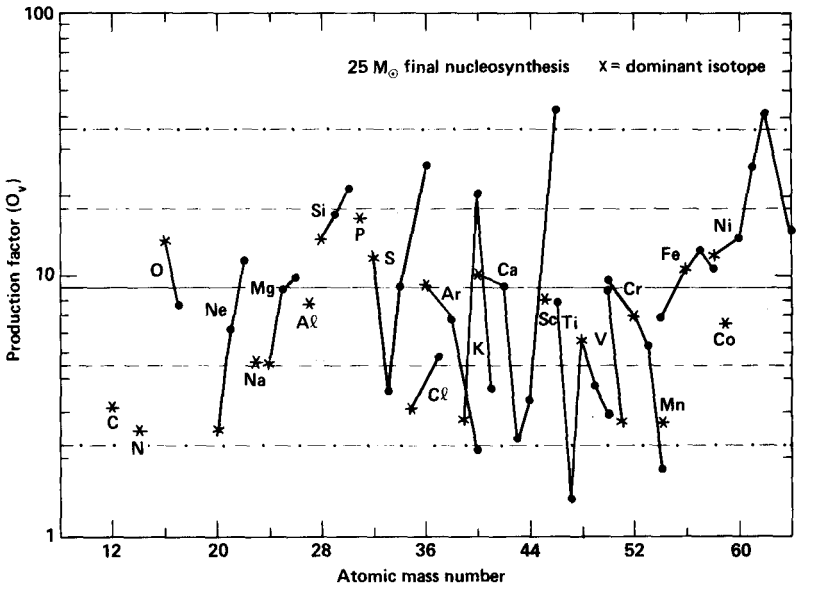

Figure 5. Isotopic nucleosynthesis in a 25 $M_\odot$ explosion. Final abundances in the ejecta are plotted for isotopes from ^{12}C to ^{64}Ni compared to their abundances in the sun (Cameron 1982). An average production factor of 9 characterizes the distribution. If one gram in 9 of the matter in the Galaxy has experienced conditions like those in a 25 $M_\odot$ star, its metallicity will resemble the sun with an abundance pattern as shown. Figure take from Woosley and Weaver (1985).

2.5 Pulsational Pair-Instability Supernovae

We have recently studied 75 and 100 $M_\odot$ model stars and found evolution in the final stages that differed markedly different from that of stars of lower mass (see also Barkat, Rakavy, and Sack 1967; Woosley and Weaver 1985, 1986a). Near the end of helium burning, the

https://doi.org/10.1017/S0252921100086048 Published online by Cambridge University Press

hydrogen envelope of each star was removed from the calculation when it became apparent that no reasonable choice of surface boundary conditions would allow it to remain bound in the presence of a luminosity that was very nearly super-Eddington and on a star prone to pulsational instability. Thus in its final stages the 75 $M_\odot$ (100 $M_\odot$) star was a 36 $M_\odot$ (45 $M_\odot$) helium core, *i.e.*, a massive Wolf-Rayet (WR) star. Removal of the envelope has no important effect on the subsequent evolution of the helium core although it obviously affects the observational properties of the star and supernova.

Following the central exhaustion of carbon and neon in burning stages that never provided a nuclear energy generation in excess of local neutrino losses, these stars encountered the electron-positron pair instability (Figs. 6 and 7) upon attempting to burn oxygen. We consider in some detail the continued evolution of the 45 $M_\odot$ helium core here. That of the 36 $M_\odot$ core remains under study but is qualitatively similar except that the pair instability is encountered later after roughly 1/2 of the oxygen has been burned in the center.

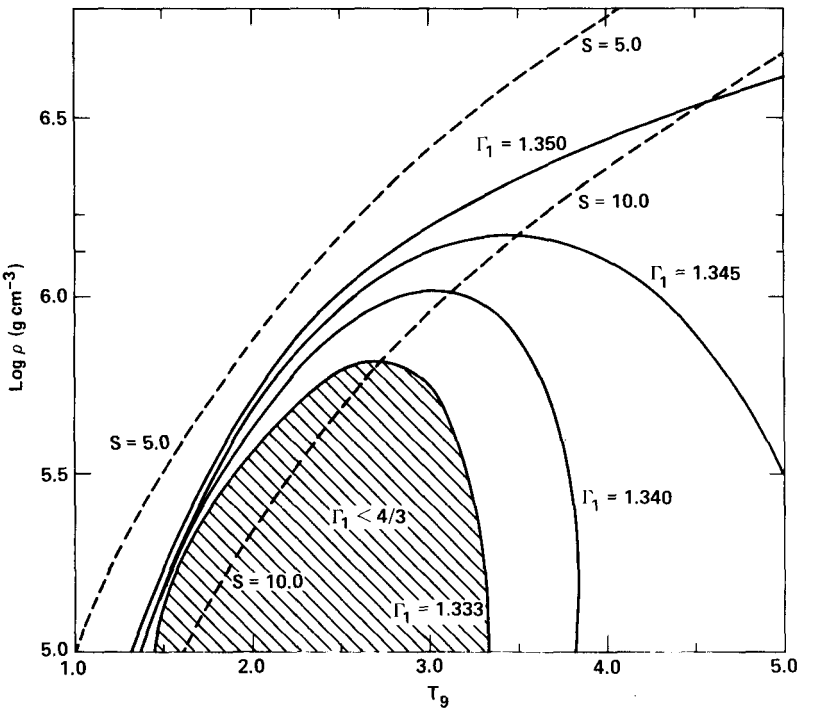

Figure 6. The structural adiabatic index, Γ_1, and dimensionless entropy, S, are shown as a function of temperature and density. The (cross-hatched) region interior to $\Gamma_1 = 4/3$ is unstable because of the energy required to create the rest mass of electron-positron pairs. At higher temperature marginal stability is restored as the leptons become relativistic, the ionic contribution keeping Γ_1 slightly greater than 4/3. Because stability is so marginal, one should include post-Newtonian corrections to gravity when modelling stars in this thermodynamic region.

The first collapse of the 45 $M_\odot$ helium core, initiated by the pair instability *prior* to oxygen ignition, reached a peak central temperature of 3.0×10^9 K and a density of 1.7×10^6 g

https://doi.org/10.1017/S0252921100086048 Published online by Cambridge University Press

cm^{-3} (with peak density occurring 30 s prior to maximum temperature). This led to explosive oxygen burning and expansion (Fig. 7). The initial explosion was far too weak to unbind the entire star, but a portion, about 1/4 $M_\odot$, was ejected from the surface at velocities of several thousand kilometers per second (2.2×10^{49} erg). The central density of the star declined to 7.4×10^4 g cm^{-3}, and roughly one month (2.96×10^6 s) long Kelvin-Helmholtz stage ensued as the star contracted and encountered the pair instability again. This time a higher peak temperature, 3.3×10^9 K, and density, 2.4×10^6 g cm^{-3}, were reached and a more violent explosion ensues, 6.5×10^{49} erg carried by an additional quarter solar mass of ejecta. The central density declines to 6.7×10^4 g cm^{-3} and the temperature to 1.0×10^9 K. For a time the star oscillates violently but eventually settles down after 3 months ($t_{tot} = 1.28 \times 10^7$ s) to encounter the pair instability a third time (Fig. 7), the peak temperature this time being 3.7×10^9 K and the peak density 6.3×10^6 g cm^{-3}. This leads to a strong explosion, by far the strongest of the group, and the ejection of 2.7 $M_\odot$ of surface material (helium, carbon, and oxygen) with energy 3.4×10^{50} erg. The core then expands, following oscillations (Fig. 8), to 1.2×10^5 g cm^{-3} and 9.8×10^8 K. Relaxation once again leads to a fourth and final pair instability and explosion at $t = 4.74 \times 10^7$ s characterized by peak conditions 2.2×10^7 g cm^{-3} and $T = 4.6 \times 10^9$ K. This explosion was a very weak one since most of the oxygen in the center had already been burned during previous episodes. In fact the inner 3 $M_\odot$ consisted almost entirely of silicon at the beginning of the fourth collapse and about 1.5 $M_\odot$ of iron group isotopes contaminated by a trace of silicon following. Expansion stabilized at 5.8×10^5 g cm^{-3} and 1.3×10^9 K and no discernible mass was ejected. On the fifth time down, 5.25×10^7 s after the onset of the first explosion *the pair instability was not encountered again*. Neutrino losses during the prior 4 episodes had led to a gradual decrease in the central entropy (Figs. 6 and 7) to the point that the unstable region was barely avoided. The collapse was therefore briefly (3 days) halted by several stages of convective (central and shell) silicon burning following which an iron core of $\sim$2.2 $M_\odot$ collapsed to nuclear density.

The continued evolution of this object is under study by Mayle and Wilson at Livermore. Its core characteristics are similar to those of an earlier 100 $M_\odot$ model examined by Wilson *et al* 1985 which at the last point calculated ($t \approx 1.3$ s after core bounce) had not achieved even a "delayed" explosion. During this one second the iron core had accreted an additional 1.1 $M_\odot$ growing from 1.85 $M_\odot$ to more than 2.95 $M_\odot$and will almost certainly become a black hole. Whether continued evolution may ultimately reveal the development of a powerful neutrino-energized supernova or, perhaps a mantle explosion owing to rotation and nuclear burning (Bodenheimer and Woosley 1983), remains to be determined. It does not seem likely to us that the entire 39 $M_\odot$ of material remaining outside the core can accrete into the black hole without some sort of violent display probably involving much greater energy than all 4 of the pulsational outbursts combined ($\sim 4 \times 10^{50}$ erg).

The optical appearance of this long duration supernova was not accurately determined in the present calculation both because of the complications introduced by the ejected matter, which was not finely zoned, and a poor representation of the low temperature opacities for helium and heavier elements. Most of the time spent in the unstable period elapsed during the various Kelvin-Helmholtz stages following explosions of the core. The luminosity during these periods was close to, though somewhat above, the Eddington value, *i.e.*, for material having Z = N and a 42 $M_\odot$ star about 10^{40} erg s^{-1}. This fairly steady luminosity was punctuated by brilliant outbursts having peak luminosity greater than 10^{42} erg s^{-1}, usually lasting for a few days, and luminosity greater than 10^{41} erg s^{-1} for a few weeks. The appearance of the supernova is greatly influenced by the fact that the star has lost nearly all of its hydrogen

envelope (here all by assumption). The thin layer (few $M_\odot$) of helium capping the oxygen mantle may also be lost in the strong stellar wind known to characterize WR stars so that at the time of its explosion the star would be a WO star. The spectrum would then be dominated by lines of oxygen. The light curve resulting from the final explosion, if there is one, would be sensitive to the amount of radioactive ^{56}Ni ejected. It is by no means certain that most of the radiation would appear in optical wavelengths.

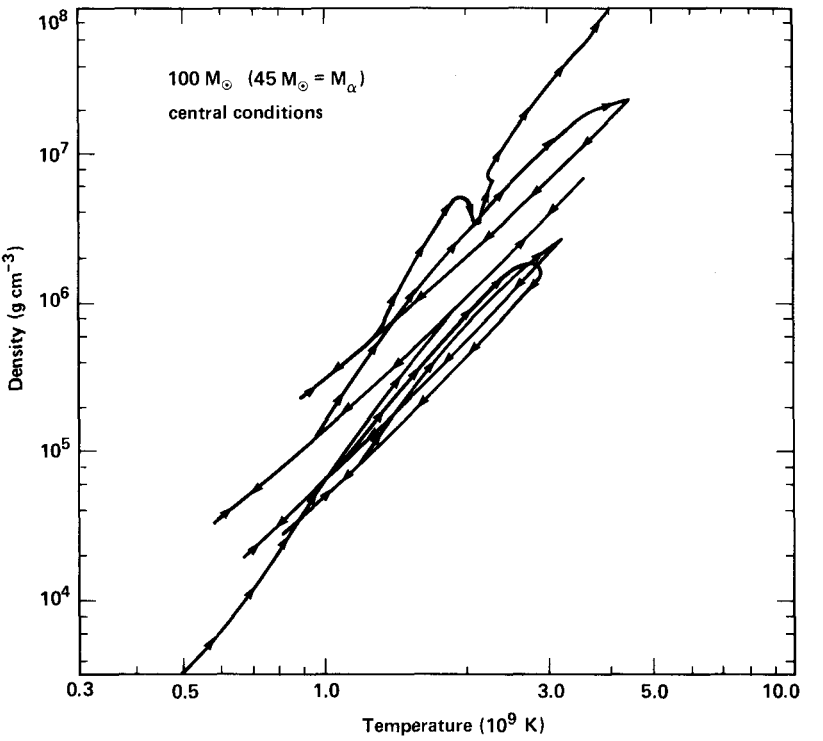

Figure 7. Temperature and density history of the center of a 45 $M_\odot$ helium star as its core encounters the pair instability upon attempting to ignite oxygen burning. After 4 violent pulsations neutrino losses have reduced the entropy to the point that the pair unstable region (Fig. 6) is avoided. Following a brief stage of hydrostatic silicon burning the core collapses to nuclear density.

Clearly a great deal more work is needed before the observable properties of this kind of explosion can be discussed with any certainty but outbursts of this sort may have been seen in SN 1961v (Branch and Greenstein 1971; Utrobin 1984) for a star that had not lost all of its hydrogen envelope and, more recently, in SN 1985f, the Filippenko-Sargent object, for a star that lost not only its hydrogen envelope but the helium layer as well.

https://doi.org/10.1017/S0252921100086048 Published online by Cambridge University Press

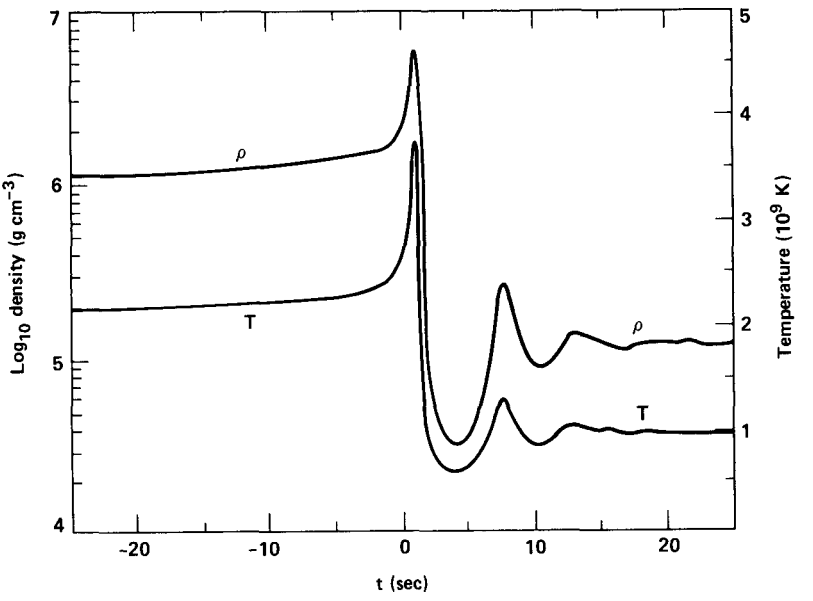

Figure 8. Temperature and density history of the center of the 45 $M_\odot$ pair unstable star as it becomes unstable for the second time. Note rapidly damped oscillations.

3. *TYPE I SUPERNOVAE*

3.1 General Comments

There are many reasons for believing that Type I supernovae occur when a white dwarf accretes a critical mass and undergoes a thermonuclear explosion. Observational evidence favors the association of such supernovae with a low mass population. They are not preferentially situated in the spiral arms of spiral galaxies (Maza and Van den Bergh 1976) and they do occur in elliptical galaxies where no Type II supernovae are seen (Tammann 1974) and no young stars are expected (although see Oemler and Tinsley 1979). Type I supernovae, by definition, lack hydrogen lines in their spectra as would be the case if a white dwarf exploded. The velocities inferred from spectral measurements of Type I's and the energies of the explosions agree with what one would obtain by converting a fraction of a white dwarf mass to iron (or ^{56}Ni). Further observational evidence supporting this inference is provided by the fact that iron is seen in the explosions (Kirshner and Oke 1975; Wu *et al.* 1983; Graham *et al* 1985) as well as the radioactive decay product of ^{56}Ni, ^{56}Co (Axelrod 1980ab; Branch 1984ab). Furthermore the degenerate nature of a white dwarf guarantees that a nuclear runaway will convert a substantial fraction of its mass to iron on a short time scale with the resulting light curve generated by the decay of these same radioactive species (Pankey 1962; Truran, Arnett, and Cameron 1967; Colgate and McKee 1969; Arnett 1979; Chevalier 1981; Weaver, Axelrod, and Woosley 1980). Finally, Type I supernovae are a very uniform class of events which might be understood if they all had a very similar origin, a compact object that creates ~0.5 to 1

https://doi.org/10.1017/S0252921100086048 Published online by Cambridge University Press

$M_\odot$ of ^{56}Ni.

Generally speaking, there are two mechanisms for the explosion: *detonation* and *deflagration*. Burning always occurs by detonation when the runaway ignites in *helium*-rich material either at the center of an accreting helium white dwarf or, off-center, at the base of an accreted helium layer on a carbon-oxygen or an oxygen-neon white dwarf. Ignition in helium occurs at sufficiently low density that burning to nuclear statistical equilibrium at $T \sim 8 \times 10^9$ generates a large local increase in the pressure, typically $\sim$5. This large overpressure leads to a shock wave. As material passes through the shock, typically at speeds of 2 to 3 times the speed of sound, the temperature and density rise, virtually instantaneously, and nuclear burning gives enough energy to keep the shock wave going. Because the expansion is supersonic, material does not have time to "get out of the way" ahead of the burning front and essentially the entire layer of helium is converted to iron group elements. Indeed, if the helium layer is massive enough and the density in the carbon-oxygen core not too high, the shock wave driven into the core may additionally propagate as a successful detonation wave in which case the star is totally disrupted and there is no bound remnant. More typically, a portion of the core stays behind as a white dwarf remnant of the supernova.

Helium detonations have been recently studied by Nomoto (1982ab) and by Woosley, Taam, and Weaver (1986). In general the models produce light curves and isotopic nucleosynthesis, especially of the iron group elements, that are in very good accord with observations and solar abundances respectively. Unfortunately the conversion of almost all of the ejected material into iron is in severe disagreement with the spectrum observed near peak light which shows (Branch 1984ab) strong absorption features of silicon, sulfur, and calcium. Helium detonations also imply higher expansion velocities and a more highly ionized iron plasma than are observed in the declining portion of the light curve (Woosley, Axelrod, and Weaver 1984). For these reasons, helium detonations are *not* presently regarded as the probable explanation for *most* Type I supernovae and greater attention is given, at least presently, to deflagrating models.

3.2 Carbon Deflagration

Deflagration occurs when an accreting carbon-oxygen white dwarf approaches the Chandrasekhar mass and ignites carbon burning in or near its center. Typical ignition conditions require a balance of neutrino losses by the plasma process and nuclear energy generation by a highly screened fusion reaction and imply $\rho \gtrsim 2 \times 10^9$ g cm^{-3}. At this high density a temperature of 8×10^9 K gives only a small increment in the large Fermi pressure, $\lesssim$20%, which is *not*, in general, large enough to propagate as a Chapman-Jouget detonation (though, as we shall see, burning may still propagate supersonically in some cases, see also Mazurek, Meier, and Wheeler 1977). Instead, once the burning front begins to travel, unburned fuel expands ahead of the front, having been notified by a sonic precursor of the events transpiring deeper in the core. Density decreases as material crosses the burning front, generates heat, and expands. Perhaps most importantly, the expansion of the outer regions of the white dwarf is rapid enough that the (subsonic) burning front never overtakes them and thus unburned fuel is ejected, as well as a portion of the star that experiences intermediate burning temperatures and produces intermediate mass elements.

Despite major successes of the carbon deflagration model for Type I supernovae, especially its good agreement with observed constraints on the spectrum (Branch *et al* 1985;

Woosley, Axelrod, and Weaver 1984) and light curve (Woosley and Weaver 1986a), there still exist major problems that suggest that our understanding is, at best, incomplete. The problems center upon the poorly determined nature of the burning front, hence gross uncertainty in the velocity with which it propagates, and the sensitivity of major results to its value. If the flame moves slowly compared to sound, then the expansion of the star is well under way before the burning front passes a fiducial point, say half-way out in mass. Thus less matter is burned to iron and, for starting points of similar gravitational binding, the supernova energy and velocity are smaller. Less ^{56}Ni produced also means a dimmer light curve, eventually, for $\lesssim 0.5$ $M_\odot$, too dim and too broad to be in accord with observations. A large flame velocity, on the other hand, gives the converse of these properties.

Uncertainty in the properties of the nuclear flame is probably the cause of a generic difficulty with deflagration models, unacceptable nucleosynthesis for the isotopes of the iron group (Woosley, Axelrod, and Weaver 1984). In the work of Nomoto, Thielemann, and Yokoi (1984), for example, ^{54}Fe/^{56}Fe is overproduced by a factor of 3.9 compared to the sun. Woosley, Axelrod, and Weaver (1984) find an even larger overproduction in a similar model. More recently recalculation by Thielemann, Nomoto, and Yokoi (1985) found an overproduction of ^{58}Ni compared to ^{56}Fe of about a factor of 5 for any reasonable value of electron capture rates. The difficulty stems from the large ignition density of the deflagrating models which leads to a great deal of electron capture during the explosion. One would like to have almost no capture since adequate ^{54}Fe (or ^{58}Ni) can be created by just those neutrons available from conversion of the initial metallicity of the star to ^{22}Ne. In fact, ^{54}Fe/^{56}Fe resulting from nuclear statistical equilibrium *with no electron capture* is about 0.05 (Z/0.015), *i.e.*, about solar for solar metallicity. Perhaps those white dwarfs that make Type I supernovae are metal deficient, but obviously the amount of electron capture must be kept to a minimum.

One might try to accomplish this by making the flame go faster. Then the central regions would begin to expand more quickly and would thus experience less electron capture. To test this possibility, we have recently calculated a series of three carbon deflagration models having different flame velocities (but all subsonic). Each model consisted of a 1.40 $M_\odot$ carbon oxygen white dwarf that underwent a thermonuclear runaway starting in its center when the density was 2.1×10^9 g cm^{-3} and temperature 8.5×10^8 K. The burning velocity was parametrized in an artificial fashion by limiting the rate at which the convective luminosity coupling the zone currently burning to the one just ahead could increase. Specifically the luminosity could not e-fold on a time shorter than the convective velocity could cross the next zone times a factor f. The convective velocity itself was calculated using mixing length theory but was limited to the sound speed. Factors, f, of 1.0 (Model 1), 0.5 (Model 2), and 0.2 (Model 3) were employed. We do not attempt to justify such an approach on physical grounds, it is only a numerical method for generating a variable flame speed. In reality, as we shall shortly see, this velocity is very complicated. What is most relevant in this particular study is the amount of electron capture that occurs for a given amount of iron group species synthesized.

The results of these three model calculations are given in Table 3 and Figures 9, 10, and 11. The mass of ^{56}Ni created, the expansion velocity, and the total explosion energy are, as one would expect, larger for smaller values of f, *i.e.*, faster flame velocities. Indeed the flame moved so rapidly in Model 3 (and only Model 3) that the sonic precursor to the burning front steepened into a detonation in the outer regions of the star where the density was lower. Thus the outer 0.06 $M_\odot$ as well as the inner $\sim$1.2 $M_\odot$ of the star was burned to nuclear statistical equilibrium. The rest of the star was chiefly in the form of silicon, sulfur,

argon, and calcium sandwiched between the two iron layers. Almost no unburned carbon and oxygen were ejecetd. The flame speed employed in Model 3 was a rough upper bound to what could exist in a deflagration. Anything faster would be supersonic.

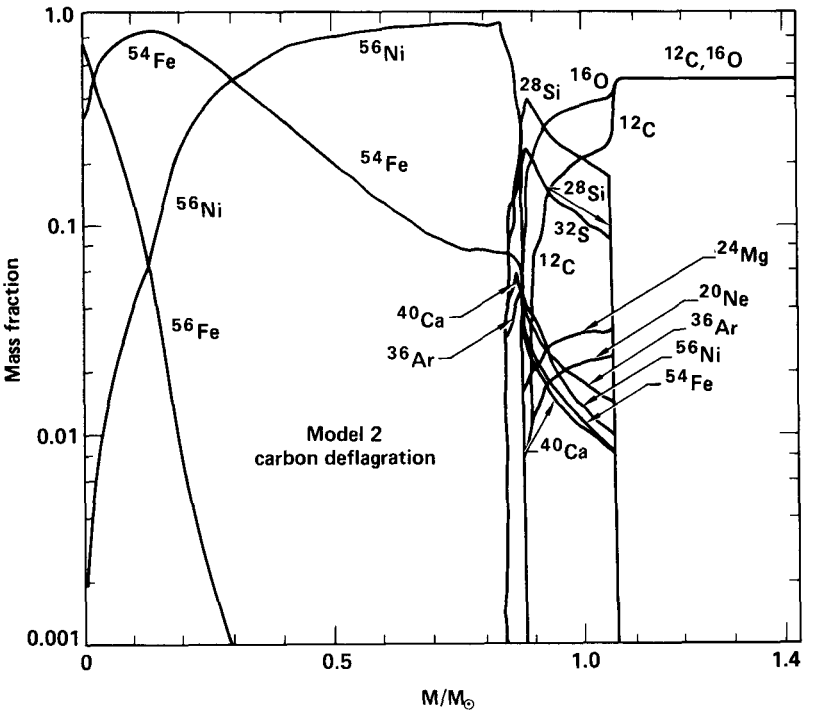

Figure 9. Final composition of a carbon deflagration supernova (Model 2).

TABLE 3
CARBON DEFLAGRATION MODELS

Model	Mass ($M_\odot$)	f	Iron ($M_\odot$)	^{56}Ni ($M_\odot$)	Y_e^c	Energy (10^{51} erg)
1	1.40	1.0	0.66	0.41	0.470	0.66
2	1.40	0.5	0.85	0.51	0.468	1.04
3	1.40	0.2	1.25	0.89	0.466	1.73

Even so, as Figure 10 and Table 3 show, the net amount of electron capture occurring during the explosion does not vary greatly from Model 1 to Model 3. Any material that has experienced nuclear statistical equilibrium characterized by an electron mole number, $Y_e \lesssim 0.49$ will be predominantly composed of ^{54}Fe, ^{58}Ni, or other neutron-rich isotopes that are even rarer in the sun (Figs. 9 and 10). Since ^{54}Fe and ^{58}Ni each have a solar abundance about 5% that of ^{56}Fe, material with $Y_e \lesssim 0.490$ can comprise no more than about 10% of

https://doi.org/10.1017/S0252921100086048 Published online by Cambridge University Press

the ejecta experiencing nuclear statistical equilibrium. Here, even in Model 3, it comprises more than 30%. This additional factor is not likely to be explained away by changes in the weak rates since the most important capture is electrons on free protons for which the rate is quite accurately known. More likely it reflects our blatant disregard for the physics of how the flame really propagates, a subject to which we now turn.

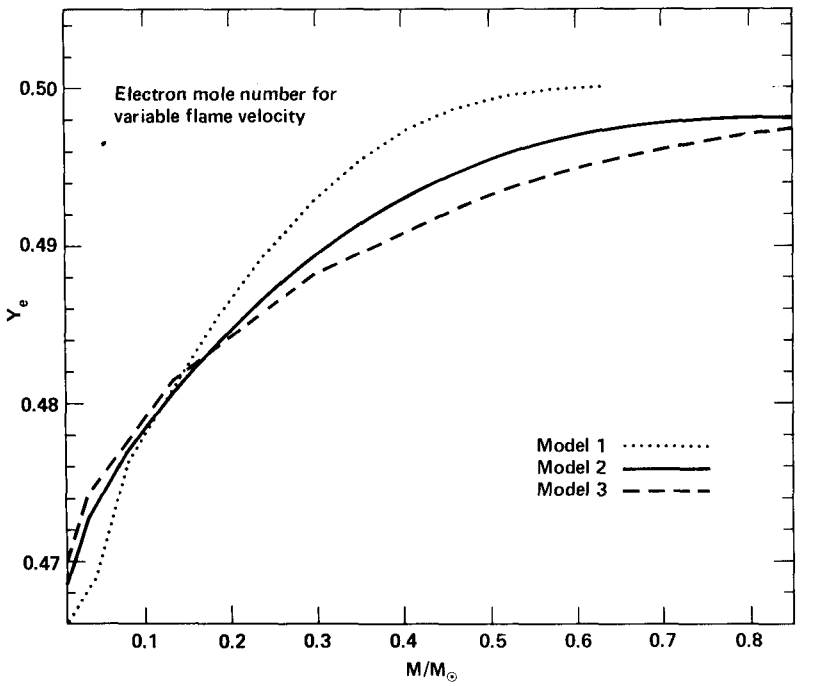

Figure 10. Distribution of the electron mole number, Y_e, in the three deflagration models. For $Y_e \lesssim 0.49$ the composition will be predominantly ^{54}Fe and ^{58}Ni, isotopes that are relatively rare in the sun.

3.3 The Physics of Degenerate Carbon Burning

There are three modes whereby the flame can physically propagate, none of which may be properly termed "convection". These are 1) conduction, 2) Rayleigh-Taylor instability, and 3) phase velocity given by initial boundary conditions. The third of these is subtle but very important. Its significance was pointed out to us by Jim Wilson. In a paper in preparation (Woosley and Weaver 1986b) each of these velocities is examined in some detail. Here the results obtained thus far will be briefly summarized.

a) The Conductive Velocity:

Following Zeldovich *et al* (1985), p. 269, the normal conductive speed of a laminar flame involving a binary reaction (here $^{12}C + {}^{12}C$) may be estimated from the mass flux equation

$$(\rho v_{cond})^2 = \frac{4\ \dot{S}_{nuc}(T_b)\,\sigma_b}{\chi_b^3\, L_e^2\, C_{vb}\,(H_b - H_o)} \qquad (5)$$

https://doi.org/10.1017/S0252921100086048 Published online by Cambridge University Press

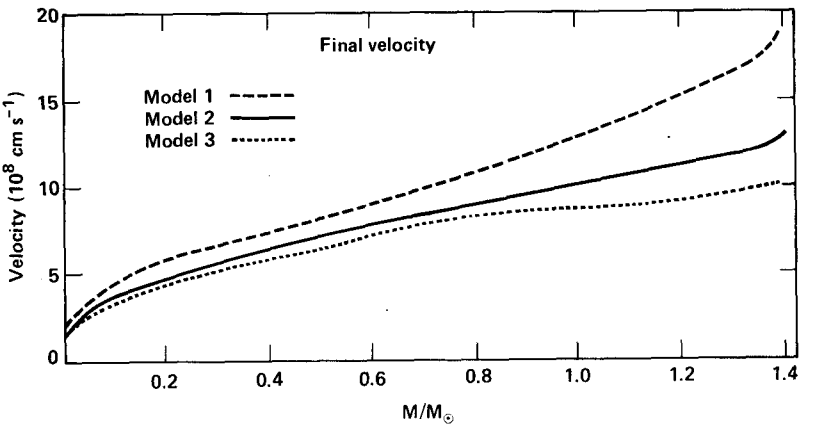

Figure 11. Final velocities of the three deflagration models.

with ρ the mass density, v_{cond} the flame speed, $\dot{S}_{nuc}$ the nuclear energy generation rate, σ the conductivity, χ a dimensionless quantity introduced in the derivation of eq. (5) in order to perform an approximate analytic integral of the nuclear energy generation rate over temperature, L_e the Lewis number, here near unity, C_v the heat capacity, and $(H_b - H_o)$ the change in enthalpy in going from the initial temperature to T_b. The quantities S_{nuc}, σ, C_v, and χ are all to be evaluated at the temperature, T_b, at which the carbon abundance goes to zero. Nuclear energy generation (given solely by the carbon burning reaction) may be approximated in a relevant temperature and density range ($9.3 \lesssim \log T \lesssim 9.8$; $8.8 \lesssim \log \rho \lesssim 9.6$) by

$$\dot{S}_{nuc} \approx 4.07 \times 10^{45} \rho_9^{1.44} X_{12}^2 \exp(-66.32/T_9^{1/3}) \text{ erg g}^{-1} \text{ s}^{-1}. \quad (6)$$

In the same temperature and density range the conductivity is

$$\sigma = \frac{4acT^3}{3\kappa_{cond}\,\rho} \approx A \rho_9^m T_9^n \quad (7)$$

with κ_{cond} the conductive opacity, $A = 3.21 \times 10^{18}$ erg s^{-1} cm^{-1} K^{-1}, $\rho_9 = \rho/(10^9$ g cm$^{-3})$, $T_9 = T/(10^9$ K), $m = 0.24$, $n = 0.95$, and the heat capacity

$$C_v \approx B \rho_9^k T_9^l \quad (8)$$

with $B = 1.57 \times 10^{16}$ erg g^{-1} $(10^9$ K$)^{-1}$, $k = -0.26$, and $l = 0.76$. The function χ normally comes from the integration of a two term expansion ("Frank-Kamenetskii approximation") of the Arrhenius exponent, $\exp -B/(kT)$, encountered in many *chemical* reactions. Since eq. (6), unlike the Arrhenius exponent, contains $T^{-1/3}$ as is more appropriate to *nuclear* reactions, our definition of χ varies from that of Zeldovich *et al*; here $\chi = 66.32\,(T_{9b} - T_{9o})/(3\,T_{9b}^{4/3})$. For cases of interest T_{9o}, the initial temperature, will be negligible compared to T_{9b}. From computer models of deflagrating white dwarfs we find, starting initially from a mass fraction 0.5, that the carbon abundance declines to 6% at 6×10^9 K and to 0.8% at 7×10^9 K and $(H_b - H_o) = 1.5 \times 10^{17}$ erg g^{-1}. Evaluating eq. (5) at a density of 2×10^9 g cm^{-3} and carbon depletion temperature $T_b = 7 \times 10^9$ K, we find $v_{cond} \sim 30$ km s^{-1}. This speed should scale as $\rho^{0.47}$.

https://doi.org/10.1017/S0252921100086048 Published online by Cambridge University Press

Equation (5) presumes that the flame propagation speed is determined entirely by the carbon burning reaction. At temperatures higher than 6×10^9 K other fuels, especially oxygen and neon will burn releasing more energy and raising the temperature. A final temperature, 8 to 9×10^9 K, characterizes the nuclear statistical equilibrium that is finally achieved. Woosley and Weaver (1986b) show, however, that the temperature at which nuclear energy generation begins to dominate conduction on the leading edge of the flame is much lower, $\sim 4.7 \times 10^9$ K, a region where energy generation is definitely from carbon burning. Thus propagation of the flame here is in what Zeldovich *et al* (page 404) term the "separation mode", with subsequent burning having little effect on the critical carbon burning reaction, and our use of eq. (5) is at least approximately valid. Some loss of accuracy results, however, because of the onset of oxygen burning at temperatures where carbon has not been completely depleted. Thus the energy generation at high temperature should be larger and our estimate of the flame speed is a bit small. It might be possible to include the effects of oxygen burning in eq. (5) but the increasing importance of photodisintegration makes it difficult to analytically formulate $\dot{S}_{nuc}$ with any accuracy.

Because of the approximate nature of this analytic estimate, it was deemed necessary to carry out a numerical study of the conduction speed in a degenerate carbon plasma using the KEPLER stellar evolution code (Weaver, Zimmerman, and Woosley 1978). The details of these calculations will be reported elsewhere (Woosley and Weaver 1986b), but microscopic zoning of the conductive burning front confirms the essential validity of the above estimates. At 2×10^9 g cm^{-3} the steady flame velocity is 60 km s^{-1}, at 5×10^8 g cm^{-3}, it is 25 km s^{-1}. The width of the burning front in both cases is $\sim 10^{-3}$ cm.

b) The "Turbulent" Flame Velocity

Actually since pressure increases and density decreases behind the conductive flame it will certainly be Rayleigh-Taylor unstable. The growth time for instability having wave number $k = 2\pi/\lambda$ is

$$\omega^2 = \frac{-g_{eff}\, k\, (\rho_2 - \rho_1)}{2\bar{\rho}} \tag{9}$$

with ρ_1 and ρ_2 the densities behind and ahead of the front, $\bar{\rho}$, the average density, and g_{eff}, the effective acceleration. We assume that the burning produces some overpressure, $\xi \sim 10\%$, above and beyond that required for local hydrostatic equilibrium. Thus

$$g_{eff} = \frac{-G\, M(r)\, \xi}{r^2} = \frac{-4\pi G r \rho \xi}{3} \tag{10}$$

if approximate spherical symmetry and constant density behind the front are assumed. The maximum wavelength, which will also be the deformation that propagates the burning the fastest, can be no larger than the radius of curvature of the burn front. We thus parametrize $\lambda = \alpha r$ with r the radius of the burned out region and $\alpha \lesssim 1$. A reasonable value for α might be 0.5. In reality the locus of the burning front will be angle dependent (Müller and Arnett 1982, 1985) but one can envision an angle-averaged flame, the velocity of which will be roughly given by the size of the largest instabilities divided by their growth time. Introducing an additional parameter, β, such that

$$v_{turb} = 2\pi\beta\lambda/\omega \tag{11}$$

and taking from the calculations (*e.g.*, Nomoto, Thielemann, and Yokoi 1985) $(\rho_2 - \rho_1)/\bar{\rho} \approx 0.2$, at least for the inner part of the star, one has

$$v_{turb} = 3.9(\frac{\alpha^3\beta^2}{\xi G\rho})^{1/2} r = K r. \tag{12}$$

For appropriate values of $\alpha \sim 0.5$, $\beta \sim 0.5$, $\xi \sim 0.1$, and $\rho \sim 10^9$ g cm^{-3}, $v_{turb} \sim 0.25 r$ cm s^{-1}. Comparing this to $v_{cond} \sim 60$ km s^{-1} we find that the flame will be propagated by conduction for $r \lesssim 2.5 \times 10^7$ cm, but after the burning encompasses a larger volume the turbulent mode of propagation will take over.

Of course other arbitrary choices for parameters could easily have led to an answer perhaps a factor of 10 different, and the above is really no more than dimensional analysis. Correct values will ultimately have to be obtained either by difficult numerical experiments (Müller and Arnett 1982, 1985) or, more likely in the immediate future, by observational constraints on the Type I supernova. For example, the flame velocity cannot be so slow as to burn too little fuel to give a high velocity explosion and produce enough ^{56}Ni to power the light curve. On the other hand v_{turb} cannot become supersonic. Thus for the time being we suggest a parametrization

$$v_{turb} = F c_s (1 - \exp(-r/R_o)). \tag{13}$$

This retains, for small r, the scaling $v_{turb} \propto r$ and approaches a fraction, F, of the sound speed at large radii. Ultimately F and R_o are to be determined by observational constraints on the light cove, explosion energy, and nucleosynthesis. As initial guesses we suggest $F = 0.5$ and $R_o = 2 \times 10^7$ cm.

c) The Phase Velocity

The above considerations apply only to an explosion initiated at a point. For a core having a finite initial temperature gradient the location of the burning front will initially "propagate" simply because regions out of communication will experience nuclear runaway at comparable times (Wilson 1985b). The time scale for the acceleration of nuclear burning at temperature T (henceforth the "runaway" time scale) is given by

$$\tau_{nuc} = \left(\dot{S}_{nuc} \frac{d\dot{S}_{nuc}}{dt}\right)^{-1} = \frac{T}{j}\left(\frac{dT}{dt}\right)^{-1} \tag{14}$$

if the nuclear energy generation rate is approximated by $\dot{S}_{nuc} \approx D X_{12}^2 \rho_9^i T_9^j$ and the density is assumed constant. In the limited temperature range 0.6 to 1.2×10^9 K, which is of greatest interest here, the effects of electron screening upon the reaction rate are important and eq. (6) is not valid. A better fit is given by $D \approx 8.25 \times 10^{15}$ erg g^{-1} s^{-1}, $i = 2.79$, and $j = 22$. (The carbon burning reaction rate itself has a fit of the same form but $D = 0.982$.) Assuming times sufficiently short that energy transport is negligible and neglecting changes in the density, the time derivative of the temperature is given by eqs. (6) and (8)

$$B(l+1)\rho_9^k T_9^l \frac{dT_9}{dt} = \dot{S}_{nuc} \tag{15}$$

https://doi.org/10.1017/S0252921100086048 Published online by Cambridge University Press

and thus

$$\tau_{nuc} = 0.152\, T_9^{-20.2}\, \rho_9^{-3.05}\ \mathrm{s} \tag{16}$$

The "phase velocity" of the front, or how its location changes with time as a result of initial conditions is given by

$$\begin{aligned} v_{phase} &= \left(\frac{d\tau_{nuc}}{dr}\right)^{-1} \\ &= 3.26 \times 10^8\, T_9^{21.2}\, \rho_9^{3.05} \left(\frac{dT}{dr}\right)^{-1} \mathrm{cm\ s^{-1}}. \end{aligned} \tag{17}$$

Thus the phase velocity is very sensitive to the temperature at which the runaway starts and is inversely proportional to the temperature gradient, an obvious limit being an infinite phase velocity if the core were exactly isothermal (see also Mazurek, Meier, and Wheeler 1977; Mazurek, Truran, and Cameron 1974). Here the temperature gradient is to be evaluated when the runaway becomes localized, *i.e.*, τ_{nuc} is short compared to both the conduction and convective energy transport time scales.

An important critical value is given by setting the phase velocity equal to the sound speed, typically about 10,000 km s^{-1} ahead of the burning front

$$\left(\frac{dT}{dr}\right)_{sonic} \lesssim 0.3\, T_9^{21.2}\, \rho_9^{3.05}\ \mathrm{K\ cm^{-1}}. \tag{18}$$

A region having an actual temperature gradient smaller than this will run away on less than a sound crossing time, thus its expansion will be supersonic in the unburned medium. For typical conditions set up by convection just prior to the runaway in various models $\rho_9 \sim 2 - 4$; $T_9 \sim 0.7 - 0.9$; $(dT/dr) \sim 1 - 10$ K cm^{-1}, $v_{phase} \sim 10^7 - 10^9$ cm s^{-1}. This spans the range of the conductive and turbulent velocities derived above and it is in part the similarity of all these velocities (as well as the sound speed) that makes the study of degenerate carbon ignition such a complex problem. We note that for a relatively large value of the central temperature (say $T \gtrsim 10^9$ K) and a shallow temperature gradient ($dT/dr \lesssim 10$ K cm^{-1}) over a substantial fraction of the inner region of the star, the conductive dominated stage of nuclear burning may be bypassed altogether and the explosion proceed directly to a turbulent propagation mode. In more extreme cases, detonation of a large fraction of the star may occur.

3.4 Carbon Deflagration Again

The discussions of the previous section suggest several possible outcomes of degenerate carbon ignition, with the choice critically sensitive to the temperature distribution that exists when the runaway commences. These outcomes are 1) complete detonation, 2) partial detonation followed by turbulent burning, and 3) conduction followed by turbulent burning.

The first possibility is favored by a high central temperature and a nearly isothermal temperature gradient. For any reasonable temperature gradient there will always be *some* region that runs away in less than a sound crossing time, but if the "detonator" is too small geometrical dilution will kill the shock before it goes very far (Sugimoto and Nomoto 1980).

Second the detonator may be large enough to get a shock wave started and burn an appreciable fraction of the star, yet the shock may die when it reaches cooler outlying regions

https://doi.org/10.1017/S0252921100086048 Published online by Cambridge University Press

where the energy that must be provided to get the fuel to burn on a Courant time scale is larger. This is the sort of behavior studied by Mazurek, Meier, and Wheeler (1977). What they overlooked, however, is that once the shock dies the burning will still propagate at a fraction of the speed of sound in the "Rayleigh-Taylor" or "turbulent" mode (eq. 13). This sort of model has the attractive feature of reducing electron capture in the central regions by rapid expansion while still retaining the intermediate mass element nucleosynthesis that renders the deflagration model so spectroscopically appealing. We are currently calculating a model of this variety. A detonation wave induced by allowing the central ignition temperature to approach $\sim 1.2 \times 10^9$ K in a CO-dwarf having similar initial conditions to Models 1 to 3 has propagated through 0.7 $M_\odot$ before dying.

Third, if the runaway commences, *i.e.*, becomes localized to the extent that burning time is less than sound crossing time, in a region with a relatively steep temperature gradient and low characteristic temperature, conduction may win for a time before sufficiently large wavelength Rayleigh-Taylor instabilities can grow and take over the flame propagation.

The actual temperature distribution and who wins depends upon the point at which one relinquishes a mixing length theory of convection in the pre-explosive evolution. If an adiabatic temperature gradient is artificially maintained while the central temperature rises to an arbitrarily high value, detonation will occur. In fact, convection cannot occur on a time scale shorter than the reciprocal of the Brundt-Väisälä frequency, essentially the time for a convective blob to move a pressure scale height. Our numerical models indicate that this occurs when the burning time becomes shorter than about 100 s, *i.e.*, at about 7×10^8 K (see also Nomoto, Thielemann, and Yokoi 1985). At such a low temperature, eq. (18) suggests that the region that burns supersonically will be very small.

Thus, pending further study, we currently favor the third possibility, a runaway that is initially slowly propagated by conduction then switching, at a radius $\sim 10^7$ cm after a second or so, to an accelerating turbulent mode with speed given by eq. (13) (see also Mazurek, Colgate, and Buchler 1980 though our numerical estimates differ substantially due to numerical error in their work). This has interesting implications for the electron capture problem. Because the structural adiabatic index of the white dwarf is so nearly 4/3, the burning of only a small amount of carbon and oxygen, say a few hundredths of a solar mass, deposits sufficient energy that, given adequate time, the entire white dwarf would expand to a configuration having considerably lower density. The limitation on this time is essentially several times the sound crossing time, or about 1/2 a second. The rapidly moving turbulent flame later catches up with this slowly expanding material, but because the density is now less, electron capture is greatly reduced.

We conclude with Figure 12 which shows the results of a relatively crude first attempt to simulate this behavior. In an initial model identical to Models 1, 2, and 3 of §3.2 the burning was forced to proceed at a relatively slow speed for a time 0.5 s before turning on "convection" with $f = 0.5$ as in Model 2. During this initial phase 0.035 $M_\odot$ of carbon and oxygen had burned to iron implying, at a density $\sim 2 \times 10^9$ g cm^{-3}, a flame speed of about 400 km s^{-1} (in retrospect a bit fast though substantially less than in most "deflagration" models). The effect upon the nucleosynthesis is dramatic. Neutron-rich isotopes like ^{50}Ti, ^{54}Cr, and ^{58}Fe not previously attributed to Type I supernovae are copiously produced in that small region of the star that, having been ignited by conduction, stayed very hot and dense for a long time. On the other hand the synthesis of ^{54}Fe and ^{58}Ni is reduced by the pre-expansion of the bulk of the star. The final iron mass ejected is 0.59 $M_\odot$ of which 0.44 $M_\odot$ is ^{56}Fe. Obvious problems remain, such as the large overproduction of the rare species ^{54}Cr, but these might be solved

by more careful tuning of the flame velocity and by finer zoning. We shall see.

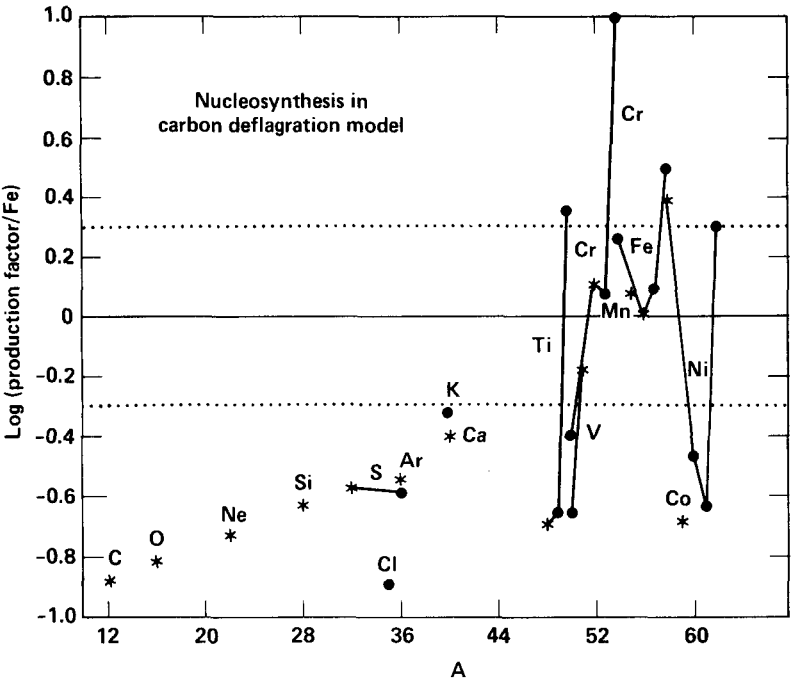

Figure 12. Isotopic nucleosynthesis in a carbon deflagration supernova in which the flame was initially constrained to propagate slowly. Though still plagued by large overproductions of rare isotopes such as ^{54}Cr, ^{50}Ti, and ^{58}Fe, the nucleosynthesis of ^{54}Fe and ^{58}Ni is improved. More careful tuning of the flame velocity may eventually alleviate these remaining overproductions. This explosion ejected 0.44 $M_\odot$ of ^{56}Fe.

This work has been supported by the National Science Foundation (AST-84-18185) and, at LLNL, by the Department of Energy through contract number W-7405-ENG-48. We thank Rob Hoffmann for help with fitting the functions given in §3.3 and Jim Wilson and Ron Mayle for helpful discussions of delayed Type II supernova explosions and degenerate carbon ignition.

REFERENCES

Arnett, W. D. 1979, *Ap. J. Lett.* 230:L37.

_____. 1983, *Ap. J. Lettr.* 263:L55.

_____. 1985, Preprint Enrico Fermi Inst., Univ. Chicago, submitted to *Ap. J. Lettr.*

Axelrod, T. S. 1980a, Ph.D. Thesis UCSC, available as UCRL preprint 52994 from Lawrence Livermore National Laboratory.

_____. 1980b, *Type I Supernovae*, ed. J. C. Wheeler. Austin: Univ. of Texas. p. 80.

Barkat, Z., Rakavy, G., and Sack, N. 1967, *Phys. Rev. Lettr.* 19:379.

Barkat, Z., Reiss, Y., and Rakavy, G. 1974, *Ap. J. Lettr.* 193:L21.

Baron, E., Cooperstein, J., and Kahana, S. 1985a, *Phys. Rev. Lettr.* 55:126.

_____. 1985b, *Nucl. Phys.*, A440:744.

Baron, E., Brown, G. E., Cooperstein, J., and Prakash, M. 1985, Preprint.

Berteli, G., Bressan, A. G., and Chiosi, C. 1984, *Astron. and Ap.* 130:279.

_____. 1985, *Astron. and Ap.* 150:33.

Bethe, H. A. 1985, private communication.

Bethe, H. A., and Wilson, J. R. 1985, *Ap. J.* 295:14.

Bodenheimer, P., and Woosley, S. E. 1983, *Ap. J.* 269:281.

Bowers, R. L. 1985, private communication.

Bowers, R. L., and Wilson J. R. 1982, *Ap. J.* 263:366.

Branch, D. 1984a, *Ann. N. Y. Acad. Sci.* 422:186.

Branch, D. 1984b, *Stellar Nucleosynthesis,* eds. C. Chiosi and A. Renzini. D. Reidel: Dordrecht. p. 19.

Branch, D., and Greenstein, J. L. 1971, *Ap. J.* 167:89.

Branch, D., Doggett, J. B., Nomoto, K., and Thielemann, F. -K. 1985, *Ap. J.*, 294:619.

Brown, G. E., Bethe, H. A., and Baym, G. 1982, *Nucl. Phys.* A375:481.

Bruenn, S. W. 1985, *Ap. J. Suppl.* 58:771.

Burrows, A. and Lattimer, J. M. 1985, *Ap. J.*, in press.

Cameron, A. G. W. 1982, *Essays in Nuclear Astrophysics*, ed. C. Barnes, D. Clayton, and D. Schramm, Cambridge Univ. Press: Cambridge, p. 23.

Chevalier, R. A. 1976, *Ap. J.* 208:826.

_____. 1981, *Ap. J.* 246:267.

Chiosi, C. 1981, *The Most Massive Stars*, ESO Workshop, ed. S. D'Odorico, D. Baade, and K. Kaeyer. ESO: Garching. p. 27.

Colgate, S. A., and McKee, C. 1969, *Ap. J.* 157:623.

Conti, P. S., Leep, E. M., and Perry, D. N. 1983, *Ap. J.* 268:228.

Filippenko, A. V., and Sargent W. L. W. 1985, *Nature.* 316:407.

Firmani, C. 1982, In *WR Stars: Observations, Physics, and Evolution*, IAU Colloq. 99, ed. C. deLoore and A. J. Willis, p. 499.

Graham, J. R., Meikle, W. P. S., Allen, D. A., Longmore, A. J., and Williams, P. M. 1985, *M.N.R.A.S.* In press.

Hartmann, D. H., Woosley, S. E., and El Eid, M. 1985, *Ap. J.* 297:837.

Hillebrandt, W. 1984, *Ann. N. Y. Acad. Sci.* 422:197.

_____. 1985, To appear in *Cosmogonical Processes*, proceedings of A. G. W. Cameron's 60th Birthday symposium, Boulder, Colorado.

Hillebrandt, W., Nomoto, K., and Wolff, R. G. 1984, *Astron. Ap.* 133:175.

Humphreys, R. M. 1984, *Observational Tests of the Stellar Evolution Theory*, IAU Proc. 105, ed. A. Maeder and A. Renzini, D. Reidel: Dordrecht, p. 279.

Iben, I. 1985, *Quart. J. Roy. Astron. Soc.* 26:1.

Iben, I. Jr., and Renzini, A. 1983, *Ann. Rev. Astron. and Ap.* 21:271.

Iben, I., Jr. and Tutukov, A. V. 1984, *Ap. J. Suppl. Ser.* 54:335.

_____. 1985, *Ap. J. Suppl.* 58:661.

Kirshner, R. P., and Oke, J. B. 1975, *Ap. J.* 200:574.

Lamers, H. J., De Groot, M., and Cassatella, A. 1983, *Astron. and Ap.* 123:L8.

Langanke, K. and Koonin, S. E. 1983, *Nucl. Phys. A.* 410:334.

_____. 1985, *Nucl. Phys. A.* In press.

Maeder, A. 1984, *Observational Tests of Stellar Evolution Theory*, ed. A. Maeder and A. Renzini, IAU Symp. 105. D. Reidel: Dordrecht. p. 299.

Massey, P. 1981, *Ap. J.* 246:153.

Mayle, R. 1985, Ph.D. thesis, UC Berkeley.

Maza, J., and van den Bergh, S. 1976, *Ap. J.* 204:519.

Mazurek, T. J., Truran, J. W., and Cameron, A. G. W. 1974, *Ap. Space Sci.* 27:261.

Mazurek, T. J., Meier, D. L., and Wheeler, J. C. 1977, *Ap. J.* 213:518.

Mazurek, T., Colgate, S. A., and Buchler, J. R. 1980, *Jour. de Physique Colloque.* C2:159.

Meyerott, R. E. 1980, *Ap. J.* 239:257.

Müller, E., and Arnett, W. D. 1982, *Ap. J. Lett.* 261:L109.

_____. 1985, *Ap. J.*, in press.

Nomoto, K. 1982a, *Ap. J.* 253:798.

_____. 1982b. *Ap. J.* 257:780.

_____. 1984a, *Ap. J.* 277:791.

_____. 1984b, *The Crab Nebula and Related Supernova Remnants*, ed. M. Kafatos and R. B. C. Henry, Cambridge Univ. Press: Cambridge. In press.

_____. 1985, *Proceedings of the 12th Texas Symposium on Relativistic Astrophysics*, *Ann. N. Y. Acad. Sci.*, in press.

Nomoto, K., Thielemann, F. -K., and Yokoi, K. 1984, *Ap. J.* 286:644.

Oemler, A., and Tinsley, B. M. 1979, *Astron. J.* 84:985.

Pankey, T. 1962, Ph.D. Thesis Howard Univ., *Diss. abstr.* 23:4.

Pinto, P. A., and Axelrod, T. S. 1986, in preparation for *Ap. J.*

Romanishin, W., and Angel, J. R. P. 1980, *Ap. J.* 235:992.

Schild, R., and Maeder, A. 1983, *Astron. and Ap.* 130:237.

Sugimoto, D., and Nomoto, K. 1980, *Space Sci. Rev.* 25:155.

Tammann, G. A. 1974, in *Supernovae and Supernova Remnants* ed. C. B. Cosmovici. D. Reidel: Dordrecht. p. 155.

_____. 1982, *Supernovae: A Survey of Current Research,* ed. M. J. Rees and R. J. Stoneham. D. Reidel: Dordrecht. p. 371.

Thielemann, F. -K., Nomoto, K., and Yokoi, K. 1985, *Astron. and Ap.*, in press.

Truran, J. W., Arnett, D., and Cameron, A. G. W. 1967, *Canadian J. Phys.* 45:2315.

Tuchman, Y., Sack, N., and Barkat, Z. 1979, *Ap. J.* 234:217.

Utrobin, V. P. 1984, *Ap. and Spac. Sci.* 98:115.

Weaver, T. A., Axelrod, T. S., and Woosley, S. E. 1980, *Type I Supernovae*, ed. J. C. Wheeler. Austin: Univ. of Texas. p. 113.

Weaver, T. A., Zimmerman, G . B., and Woosley, S. E., 1978, *Ap. J.* 225:1021.

Weaver, T. A., Woosley, S. E., and Fuller, G. M. 1985, *Numerical Astrophysics*, ed. J. Centrella, J. LeBlanc, and R. Bowers. Jones and Bartlett: Boston. p. 374.

Webbink, R. F. 1984, *Ap. J.* 277:355.

. Weidemann, V., and Koester, D. 1983, *Astron. and Ap.* 121:77.

Wilson, J. R. 1985a, *Numerical Astrophysics*, ed. J. M. Centrella, J. M. LeBlanc, and R. L. Bowers, (Jones and Bartlett: Boston), p. 422.

_____. 1985b, private communication.

Wilson, J. R., Mayle, R., Woosley, S. E., and Weaver, T. A. 1985, *Proc. of Twelfth Texas Symp. on Rel. Ap., Ann. N. Y. Acad. Sci.*, in press.

Woosley, S. E., Axelrod, R. S., and Weaver, T. A. 1984, *Stellar Nucleosynthesis,* ed. C. Chiosi and A. Renzini, (D. Reidel: Dordrecht), p. 263.

Woosley, S. E., and Weaver, T. A. 1982a, *Supernovae: A Survey of Current Research*, ed. M. J. Rees and R. J. Stoneham, D. Reidel: Dordrecht, p. 79.

_____. 1982b, *Essays in Nuclear Astrophysics*, eds. C. A. Barnes, D. D. Clayton, and D. N. Schramm, Cambridge Univ. Press: Cambridge, p. 377.

_____. 1985, *Nucleosynthesis and Its Implications On Nuclear and Particle Physics*, Proc. Fifth Moriand Astrohysics Conference, ed. J. Audouze and T. van Thuan, D. Reidel: Dordrecht, in press.

_____. 1986a, *Ann. Rev. Astron. and Ap.*, in press.

_____. 1986b, in preparation for *Ap. J.*.

Woosley, S. E., Weaver, T. A., and Taam, R. E. 1980, *Type I Supernovae*, ed. J. C. Wheeler, Austin: Univ. of Texas, p. 96.

Woosley, S. E., Taam, R. E., and Weaver, T. A. 1986, *Ap. J.*, 301:000.

Wu, C. -C., Leventhal, M., Sarazin, C. L., and Gull, T. R. 1983, *Ap. J. Lett.* 269:L5.

Zeldovich, Ya. B., Barenblatt, G. I., Librovich, V. B., and Makhviladze, G. M. 1985, *The Mathematical Theory of Combustion and Explosions*, Plenum Publ. Corp.: New York.

Discussion:

R. Blandford: If the prompt explosion mechanism fails in the lower mass stars [Type II supernovae], *i.e.*, the shock stalls, can one still drive the supernova through the delayed neutrino deposition mechanism? If the answer is yes, do you believe that essentially all supernovae explode in this manner?

Woosley: That would be Jim Wilson's opinion (Wilson *et al* 1985). It appears even easier for the delayed energy transport to produce an explosion in the 9 to 15 $M_\odot$ range because of the rapid fall off of density outside the iron core. Thus the explosion occurs in a shorter time and following the accretion of less matter. As I cautioned, however, the general validity of the delayed mechanism is still debated, *eg.* by Arnett and Hillebrandt. Others such as Bethe, Baron, and Hillebrandt still believe that a *prompt* explosion *will* occur in this mass range.

R. Klein: Is the mechanism by which the neutrino flux gives renewed life to the stalled shock energy or momentum deposition? How efficiently do the neutrinos deposit in the shock which I presume is relatively optically thin?

Woosley: It is *energy* deposition. Roughly 1% of the energy in the streaming neutrino flux deposits in the optically thin material beneath the shock. Any mechanism that boosts this flux, *e.g.* convection, will increase the energy of the explosion.

B. Stein: What leads to detonations in helium [as opposed to] deflagrations in carbon and oxygen?

Woosley: Helium ignites at a lower temperature and thus at a lower density. Since the complete combustion of either helium or carbon and oxygen yields comparable temperatures in nuclear statistical equilibrium, ~ 8 to 9×10^9 K, the change in pressure (sometimes referred to as the *overpressure*) will be greater for the case that was initially less degenerate, *i.e.*, helium. A larger overpressure favors a detonation wave which otherwise left to itself would die of geometrical dilution. In some cases it is also possible for detonation to occur in a CO-core as I have discussed.

F. Shu: Do I understand correctly that the preferred models for Type I supernovae do not leave neutron stars and therefore that the neutron stars found in globular clusters (as x-ray sources) must originate by some other process.

Woosley: Any explosion that would be called a normal "Type I" on the basis of its light curve and spectrum would not leave a neutron star (though in some cases it could leave a white dwarf). Similar circumstances to those invoked for Type I supernovae, *e.g.* accretion onto an oxygen-neon dwarf or even accretion at the Eddington rate onto a CO-dwarf, could lead to the direct collapse of the white dwarf to a neutron star, but then the optical display, if any, would not resemble a Type I supernova. The collapse of the cores of massive stars, on the other hand, seems likely to give neutron stars.

V. Icke: There is observational evidence - *e.g.* from Kennikutt's H_α observations, and from the occurrence of massive stars in white dwarf containing associations - that stars more massive than 6 - 7 $M_\odot$ do not form white dwarfs. Can you comment on what might make such a lowish mass star explode?

Woosley: The lower mass limit for stars that develop thin helium shells and degenerate carbon oxygen cores is somewhat uncertain. Here I have adopted 9 $M_\odot$ as is common in the present literature. This value is sensitive to, among other things, the theory of convective

https://doi.org/10.1017/S0252921100086048 Published online by Cambridge University Press

overshoot employed in the stellar model calculations. Berteli, Bessan, and Chiosi (1985) suggest that a much lower mass, even lower than 6 $M_\odot$, might be appropriate. Then the behavior I have described for "9 to 15 $M_\odot$" stars would be shifted downwards. On the other hand, if the formation of a thin helium shell did not lead to envelope ejection (Tuchmann, Sack, and Barkat 1979) and white dwarf formation, the degenerate carbon core would eventually grow to the Chandrasekhar mass and explode much as I have described for carbon deflagrations models of Type I supernovae. Since the star would still have an extended hydrogen envelope the supernova would be Type II however, characterized by an exponential tail produced by radioactive decay (see also Iben and Renzinni 1983).

R. Blandford: Would you comment on the iron production problem in the white dwarf deflagration model of Type I supernovae?

Woosley: There is a problem with *any* source of iron (or other heavy elements) in our Galaxy that if nucleosynthesis occurs at a constant rate, *i.e.*, was not much greater when the Galaxy was forming, then the average rate required to produce present abundances in stars would *overproduce* iron by a factor of roughly 5 to 10 in the much less massive interstellar medium (and thus in young newly forming stars) if the ISM has been a closed system for the last several billion years. Specifically, if Type I supernovae produce 0.5 $M_\odot$ of iron every 36 years, then there would obviously be considerably more than a solar abundance of iron ($X = 10^{-3}$) in the ISM with mass $\sim 10^{10}$ $M_\odot$ after a billion years. Possible resolutions that have been suggested are (1) mass infall into our Galaxy, (2) that a portion of the iron escapes from the Galaxy, and/or (3) that the present Type I supernova rate is considerably less than Tammann estimates. See Woosley, Taam, and Weaver (1986) for further discussion. It is worth noting that even though they involve a low mass population, Type I's may have occurred at a greatly accelerated rate when the Galaxy was forming, or maybe Type II's dominated in iron synthesis then. It is a complicated issue but not necessarily one that speaks ill of the deflagration model.

V. Icke: I wonder what of this might be applicable to the first generations of stars in the universe. Can you say a few words about what explosion mechanisms are relevant to low metallicity, low helium stars?

Woosley: First, though others may differ, I do not expect helium to have changed appreciably (more than $\sim 5\%$ by mass say) since the Big Bang. For simplicity in answering your question I shall also assume a constant initial mass function (IMF). The metallicity affects the optical appearance of the presupernova star and of the supernova, both being more compact at the time of explosion. Zero metallicity and a diminished helium abundance also affects the stellar mass range that leaves white dwarfs as opposed to supernova (Iben and Renzini 1983) and the main sequence mass - helium core mass relation (Table 1). Other than that things are pretty much as I have described. A helium core of given mass will have the same advanced evolution regardless of its initial metallicity as will an accreting white dwarf. Some details of the nucleosynthesis will be altered.

M. Shull: Regarding zero-metallicity star formation [and the IMF] recent calculations (Palla *et al*; Shull 1984) show that cooling by H_2 can lower the Jean's mass to below 1 $M_\odot$. Thus Silk's original arguments about the lack of metal cooling probably don't apply.

Woosley: I agree. But there may be other ways in which the metallicity influences the IMF, the self limitation of the growth of an accreting protostar by grain opacity for example.

https://doi.org/10.1017/S0252921100086048 Published online by Cambridge University Press